

## ORIGINAL ARTICLE

# miR-125a-5p in astrocytes attenuates peripheral neuropathy in type 2 diabetic mice through targeting TRAF6



Aziguli Kasimu<sup>a</sup>, Xierenguli Apizi<sup>a</sup>, Dilibaier Talifujiang<sup>a</sup>, Xin Ma<sup>a</sup>, Liping Fang<sup>b</sup>, Xiangling Zhou<sup>c,\*</sup>

<sup>a</sup> Department of Pain Treatment, People's Hospital of Xinjiang Uygur Autonomous Region, Urumqi City, Xinjiang Uygur Autonomous Region 830001, China

<sup>b</sup> Department of Endocrinology, Honghu People's Hospital, Jingzhou City, Hubei Province 433200, China

<sup>c</sup> Department of Neurology, Puren Hospital Affiliated to Wuhan University of Science and Technology, Wuhan City, Hubei Province 430081, China

Received 23 November 2020; accepted 14 January 2021

Available online 3 May 2021

## KEYWORDS

miR-125a-5p;  
TRAF6;  
Astrocytes;  
Diabetic mice;  
Diabetic peripheral  
neuropathy

## Abstract

**Introduction:** Elimination or blocking of astrocytes could ameliorate neuropathic pain in animal models. MiR-125a-5p, expressed in astrocyte derived extracellular vesicles, could mediate astrocyte function to regulate neuron communication. However, the role of miR-125a-5p in DPN (diabetic peripheral neuropathy) remains elusive.

**Materials and methods:** Type 2 diabetic mouse (db/db) was used as DPN model, which was confirmed by detection of body weight, blood glucose, mechanical allodynia, thermal hyperalgesia, glial fibrillary acidic protein (GFAP) and monocyte chemoattractant protein-1 (MCP-1). Astrocyte was isolated from db/db mouse and then subjected to high glucose treatment. The expression of miR-125a-5p in db/db mice and high glucose-induced astrocytes was examined by qRT-PCR analysis. Downstream target of miR-125a-5p was clarified by luciferase reporter assay. Tail vein injection of miR-125a-5p mimic into db/db mice was then performed to investigate role of miR-125a-5p on DPN.

**Results:** Type 2 diabetic mice showed higher body weight and blood glucose than normal db/m mice. Thermal hyperalgesia and mechanical allodynia were decreased in db/db mouse compared with db/m mouse, while GFAP and MCP-1 were increased in db/db mouse. High glucose treatment enhanced the protein expression of GFAP and MCP-1 in astrocytes. Sciatic nerve tissues in db/db mice and high glucose-induced astrocytes exhibited a decrease in miR-125a-5p. Systemic administration of miR-125a-5p mimic increased mechanical allodynia and thermal hyperalgesia, whereas it decreased GFAP and MCP-1. TRAF6 (tumor necrosis factor receptor associated factor 6) was validated as target of miR-125a-5p.

\* Corresponding author.

E-mail address: [zhouxiangling1123@163.com](mailto:zhouxiangling1123@163.com) (X. Zhou).

<https://doi.org/10.1016/j.endinu.2021.01.007>

2530-0164/© 2021 SEEN y SED. Published by Elsevier España, S.L.U. All rights reserved.

**Conclusion:** MiR-125a-5p in astrocytes attenuated DPN in db/db mice by up-regulation of TRAF6, which indicated the potential therapeutic effect.

© 2021 SEEN y SED. Published by Elsevier España, S.L.U. All rights reserved.

## PALABRAS CLAVE

miR-125a-5p;  
TRAF6;  
Astrocitos;  
Ratones diabéticos;  
Neuropatía periférica  
diabética

## miR-125a-5p en los astrocitos atenúa la neuropatía periférica en ratones con diabetes tipo 2 al actuar sobre TRAF6

### Resumen

**Introducción:** La eliminación o el bloqueo de los astrocitos podría mitigar el dolor neuropático en modelos animales. El miR-125a-5p, expresado en vesículas extracelulares derivadas de astrocitos, puede mediar en la función de los astrocitos para regular la comunicación neuronal. Sin embargo, la función de miR-125a-5p en la neuropatía periférica diabética (NPD) sigue sin estar clara.

**Pacientes y métodos:** Se usó como modelo de NPD, al ratón con diabetes tipo 2 (db/db), que se confirmó mediante detección de peso corporal, la glucemia, la alodinia mecánica, la hiperalgesia térmica, la proteína ácida fibrilar glial (GFAP) y la proteína quimiotáctica de monocitos 1 (MCP-1). Se aislaron astrocitos de ratón db/db y se sometió luego a tratamiento con glucosa elevada. Se determinó la expresión de miR-125a-5p en ratones db/db y en astrocitos inducidos por la glucosa elevada mediante análisis qRT-PCR. La diana de miR-125a-5p se aclaró mediante un ensayo de informador de la luciferasa. Se procedió luego a la inyección en la vena de la cola de imitador de miR-125a-5p en ratones db/db para investigar la función de miR-125a-5p en la NPD.

**Resultados:** Los ratones con diabetes tipo 2 mostraron mayor peso corporal y una glucemia más alta que los ratones db/m normales. La hiperalgesia térmica y la alodinia mecánica disminuyeron en los ratones db/db, en comparación con los db/m, mientras que la GFAP y la MCP-1 aumentaban en los ratones db/db. El tratamiento con glucosa elevada potenció la expresión de las proteínas GFAP y MCP-1 en los astrocitos. Los tejidos del nervio ciático de los ratones db/db y los astrocitos inducidos por glucosa elevada mostraron un descenso de miR-125a-5p. La administración sistémica de imitador de miR-125a-5p aumentaba la alodinia mecánica e hiperalgesia térmica, mientras que disminuía la GFAP y la MCP-1. Se validó TRAF6 (factor asociado con el receptor del factor de necrosis tumoral 6) como diana de miR-125a-5p.

**Conclusión:** miR-125a-5p en los astrocitos atenuó la NPD en ratones db/db mediante regulación al alza de TRAF6, lo que sugiere su posible efecto terapéutico.

© 2021 SEEN y SED. Publicado por Elsevier España, S.L.U. Todos los derechos reservados.

## Introduction

Diabetic peripheral neuropathy (DPN) is a common chronic complication of diabetes mellitus and one of the most common causes of acute or chronic pain syndrome in diabetic patients.<sup>1</sup> The main manifestations of DPN are spontaneous pain, hyperalgesia and allodynia, and autoimmune disorders, oxidative stress vascular injury, metabolic toxicity or neurotrophic factor deficiency are the main pathological mechanism of DPN.<sup>2</sup> Although neurotrophic factors supplementation, blood glucose and pressure control as well as antioxidant therapies have been applied in clinical application for treatment of DPN, patients with DPN still suffer from chronic neurogenic pain due to the complicated pathogenesis of DPN.<sup>3</sup> Therefore, molecular mechanism of DPN and effective therapeutic targets are urgently needed to attenuate neurogenic pain.

MicroRNA (miRNA) can repress gene expression and plays a regulatory role in various diseases.<sup>4</sup> Growing evidences

have indicated the pivotal role of miRNA in pathogenesis of diabetic neuropathy, suggesting potential diagnostic and therapeutic applications.<sup>5</sup> For example, research has found a negative correlation between miR-146a and the severity of DPN,<sup>6</sup> and overexpression of miR-146a could relieve DPN in type 2 diabetic mice.<sup>7</sup> Suppression of miR-25 could enhance secretion of inflammatory factors to exacerbate DPN.<sup>8</sup> MiR-125a-5p is known as a tumor suppressor in hepatocellular carcinoma,<sup>9</sup> colon cancer<sup>10</sup> and cervical cancer.<sup>11</sup> Moreover, miR-125a-5p was found to attenuate accumulation of lipid droplets, and glucose consumption and uptake in type 2 diabetes mellitus.<sup>13</sup> However, the role of miR-125a-5p in DPN remains elusive.

TRAF6 (tumor necrosis factor receptor associated factor 6) participates in various signal transduction to mediate adaptive and innate immunity, tissue homeostasis, etc.<sup>14</sup> TRAF6 is involved in susceptibility of type 2 diabetes mellitus,<sup>15</sup> and represses vascular diseases in diabetes mellitus.<sup>16</sup> Treatment of DPN could decrease TRAF6

in dorsal root ganglion neurons,<sup>17</sup> and down-regulation of TRAF6 could lead to inactivation of NF- $\kappa$ B pathway, consequently ameliorating DPN.<sup>18</sup>

Since TRAF6 has been identified as a binding target of miR-125a-5p in the regulation of LPS-induced inflammatory response<sup>19</sup> and human osteoarthritic chondrocytes,<sup>20</sup> this study hypothesized that miR-125a-5p may target TRAF6 to attenuate DPN in type 2 diabetic mice.

## Materials and methods

### Animals

Experiments involved in mice model were approved by People's Hospital of Xinjiang Uygur Autonomous Region and in accordance with European recommendations for the care and use of laboratory animals and Good Laboratory Practice. Eighteen male db/db mice (BKS.Cg-m<sup>+/+</sup>Lepr<sup>db</sup>/J) (20 weeks old, 20–25 g) and six heterozygotes mice (db/m; 8 weeks old, 20–25 g) were acquired from National Resource Center for Mutant Mice (Nanjing, China), and housed at room with 22 °C and 12/12 h light–dark cycle. The db/db mice were randomly divided into three groups: db/db, db/db +NC mimic and db/db+miR-125a-5p mimic. For administration of miRNA, 10 mg chemically modified miR-125a-5p mimic or the negative control (NC mimic) by MaxSuppressor in Vivo RNA-Lancer II (BIOO Scientific, Austin, TX, USA) were tail vein injected into db/db mice that were anesthetized under 60 mg/kg pentobarbital. The miRNA administration was performed once every four days for a total of four injections. Two days after the last injection, mice were conducted with different functional analyses. Allodynia was interpreted as pain caused by stimuli that normally do not cause pain. Therefore, stimuli that caused withdrawal response is stronger in normal mouse, and weaker in db/db mouse.

### Blood glucose and body weight

Two days after the last injection, body weight and blood glucose were measured at 08:00. Tail-prick was performed to collect blood samples from each group, and glucometer (Accu-Check Integra test strips, Roche, Germany) was used to detect the blood glucose. Body weight of mice from each group was measured by an electronic weighing scale.

### Tactile and heat responsiveness

For mechanical allodynia analysis, an automated dynamic plantar aesthesiometer (Ugo Basile, Varese, Italy) was used to record the paw mechanical withdrawal threshold (MWT) of the mice in chamber with wire mesh floor. MWT was recorded as the lowest force (g) causing rapid withdrawal of right hind paw. Each experiment was repeated for three times at an interval of 5 min to average the force. For the assessment of thermal hyperalgesia, the mice were placed in a chamber with a clear glass plate at 30 ± 1 °C. A heat source was then positioned beneath the hind paw, and paw thermal withdrawal latency (TWL) was recorded as duration (s) between start of the heat and withdrawal of the paw

by Plantar Analgesia Meter (Ugo Basile, Milan, Italy). Each experiment was also repeated three times at an interval of 5 min to average the time.

### Immunofluorescence

Carbon dioxide inhalation was used for euthanasia of the mice before tissue preparation. L4–L5 spinal cords of mice under anesthesia were harvested after transcardially perfusion with 10 mL 0.9% saline, 50 mL of 4% paraformaldehyde and 0.2% (w/v) picric acid. The spinal cord segments were fixed and cut into 20  $\mu$ m-thick sections. After pre-treatment with horse serum, the sections were incubated with mouse anti-GFAP antibody (1:200, Abcam, Cambridge, MA, USA) at 4 °C overnight. Following staining with Alexa488-conjugated goat anti-mouse secondary antibody (1:500, Abcam), slides were acquired by FV1000 fluorescence microscope (Olympus, Tokyo, Japan).

### ELISA

For in vivo experiment, L4–L5 spinal cord harvested from mice was homogenized in lysis buffer (Roche, Mannheim, Germany). Proteins were quantified by bicinchoninic acid assay (Beyotime, Beijing, China). The level of MCP-1 was determined by mouse MCP-1 ELISA kit (R & D, Minneapolis, MN, USA). For in vitro experiment, level of MCP-1 in culture medium of astrocytes was also determined by the ELISA kit following manufacturer's instructions.

### Primary astrocyte culture and treatment

Astrocytes were prepared from cerebral cortexes of post-natal day 2 mice. Cerebral hemispheres without meninges were isolated and then transferred to Hank's buffer. Then, they were cut into 1 mm pieces, the tissues were triturated and filtered through a 60  $\mu$ m nylon screen. Cell pellets were harvested through centrifugation (3000 g, 5 min). The pellets were resuspended in low-glucose DMEM medium with 10% fetal bovine serum (FBS), triturated and filtered through a 10  $\mu$ m nylon screen. Cells were plated and cultured for 10–12 days to 95% confluence. Dibutyl cAMP (0.15 mM) was added into the medium to induce differentiation. The culture medium of astrocytes was changed into Opti-MEM Reduced Serum Medium (Invitrogen, Carlsbad, CA) before transfection with miR-125a-5p mimic or NC mimic. For glucose treatment, astrocytes were cultured in DMEM medium with 5.7 mM D-glucose (NG) or 40.7 mM D-glucose (HG) for 5 days before functional assays.

### Luciferase reporter

Sequence of wild type or mutant TRAF6 3' UTR were cloned into pMIR-GLO<sup>TM</sup> Luciferase vector (Promega, Madison, WI, USA) and named as TRAF6-WT or TRAF6-MUT. HEK293T cells were co-transfected with miR-125a-5p mimic or NC mimic and TRAF6-WT or TRAF6-MUT. Forty-eight hours later, luciferase activities of each group were conducted with Dual-Luciferase Reporter Assay system (Promega).

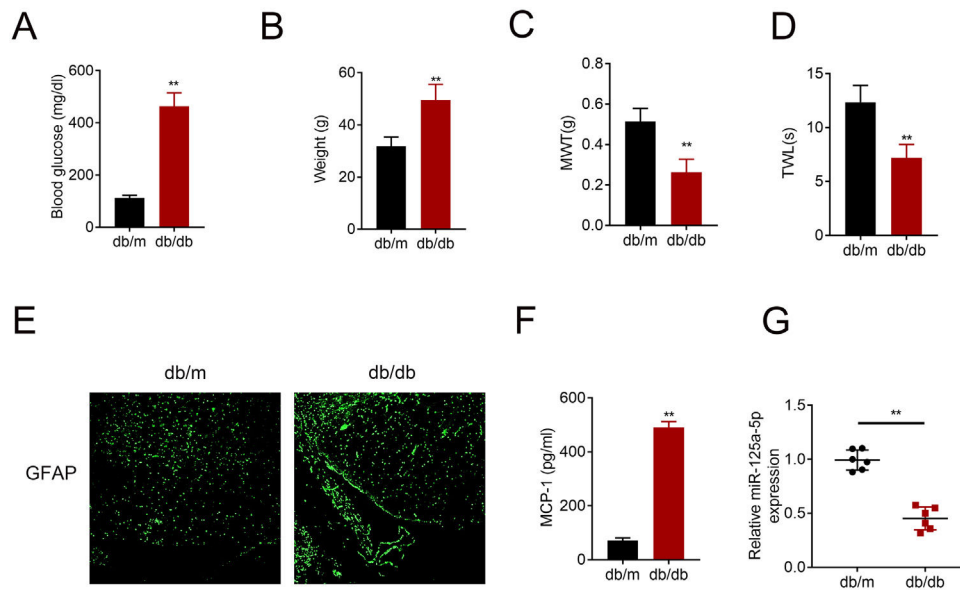


**Figure 1** MiR-125a-5p was reduced in diabetic mice. (A) Blood glucose in type 2 diabetes mice (db/db) and db/m mice. (B) Body weight of type 2 diabetes mice (db/db) and db/m mice. (C) Mechanical allodynia of type 2 diabetes mice (db/db) and db/m mice detected by MWT. (D) Thermal hyperalgesia of type 2 diabetes mice (db/db) and db/m mice detected by TWL. (E) Immunofluorescence staining of GFAP in spinal cord of type 2 diabetes mice (db/db) and db/m mice. (F) MCP-1 in type 2 diabetes mice (db/db) and db/m mice detected by ELISA. (G) Expression of miR-125a-5p in spinal cord of type 2 diabetes mice (db/db) and db/m mice detected by qRT-PCR. \*\* $p < 0.01$ . MWT: mechanical withdrawal threshold; TWL: thermal withdrawal latency; MCP-1: monocyte chemoattractant protein-1; GFAP: glial fibrillary acidic protein; ELISA: Enzyme-linked immunosorbent assay.

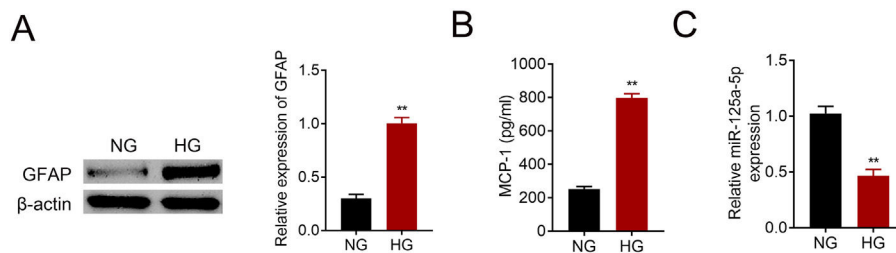


**Figure 2** MiR-125a-5p was reduced in high glucose-induced astrocytes. (A) GFAP expression in high glucose (HG) or normal glucose (NG)-induced astrocytes. (B) MCP-1 expression in high glucose (HG) or normal glucose (NG)-induced astrocytes. (C) Expression of miR-125a-5p in high glucose (HG) or normal glucose (NG)-induced astrocytes. \*\* $p < 0.01$ .

### qRT-PCR

RNAs, extracted from L4–L5 spinal cord homogenates or astrocytes via miRNeasy Kit (Qiagen, Germantown, MD), were reverse transcribed into cDNAs with M-MLV RT kit (Invitrogen). Relative expression of miR-125a-5p was determined by TaqMan microRNA assay (Thermo Fisher; Waltham, MA, USA) through the  $2^{-\Delta\Delta C_t}$  analysis. U6 was used as the internal control. The sequences of primers were listed below: miR-125a-5p (forward: 5'-GGTAAGTCACGCGGT-3' and reverse: 5'-CAGTCCGTCTCGTGGAGT-3'), and U6 (forward: 5'-CTGTTAGTACTTGGACGGGAGAC-3' and reverse: 5'-GTGCAGGGTCCGAGGT-3').

### Western blot

Proteins, extracted from L4–L5 spinal cord homogenates or astrocytes via RIPA lysis buffer, were separated and then

transferred onto a polyvinylidene difluoride membrane (EMD Millipore, Bedford, MA, USA). After blocking in 5% skim milk, membranes were incubated with primary antibodies against GFAP (1: 1500; Abcam), TRAF6 (1: 2000; Abcam), p-JNK1 (1: 2500; Abcam), p-JNK2 (1: 2500; Abcam) and  $\beta$ -actin (1: 3000; Abcam). Followed by incubation with horseradish peroxidase-conjugated secondary antibodies (1: 5000), protein signals were visualized with Super Signal West Pico Chemiluminescent Substrate kit (Thermo Fisher; Waltham, MA, USA).  $\beta$ -actin was used as the internal control.

### Statistical analysis

Data were presented as the mean  $\pm$  standard deviation, and conducted with GraphPad Prism 6.0 via Student's *t*-test or one-way analysis of variance for statistical analysis.  $p < 0.05$  was considered as statistically significant difference.

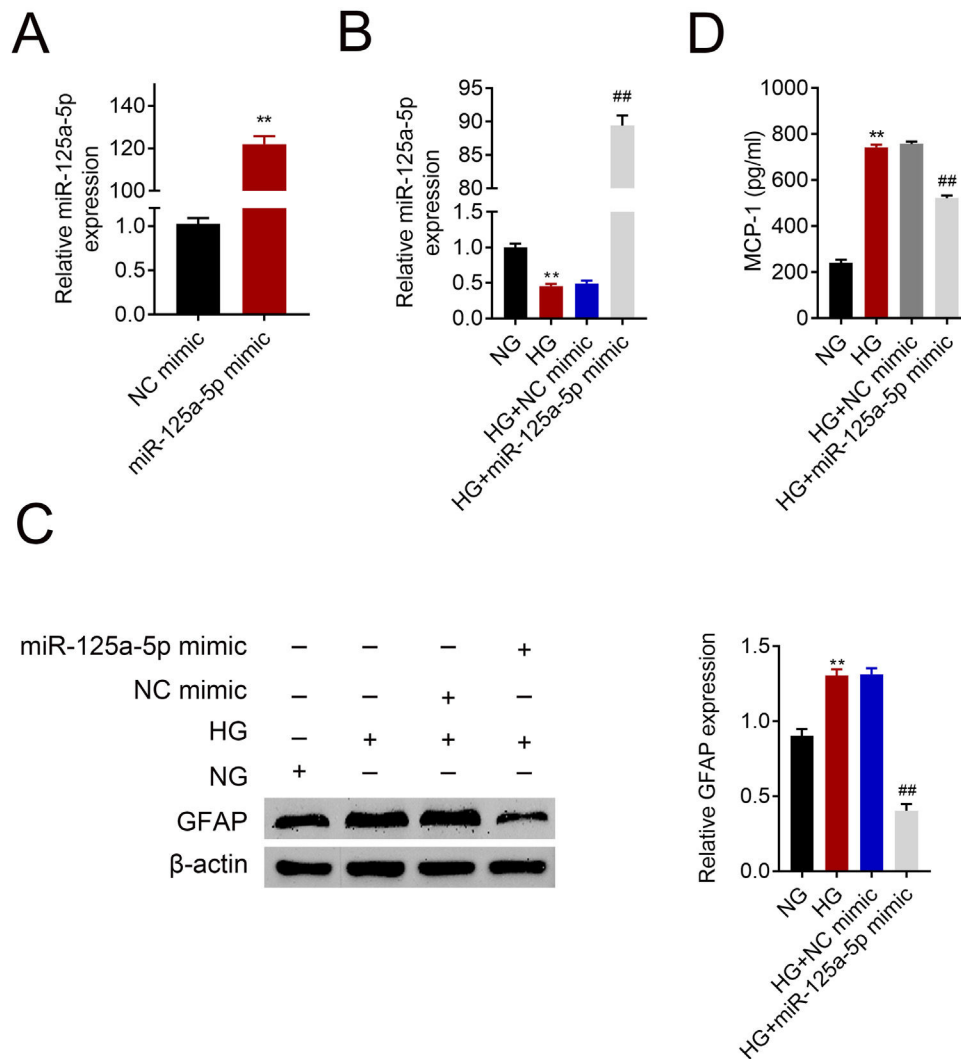


**Figure 3** Forced miR-125a-5p repressed astrocytic activation post high glucose treatment. (A) Transfection efficiency of miR-125a-5p in astrocytes. (B) Expression of miR-125a-5p in astrocytes treated with high glucose after transfection with miR-125a-5p mimic. (C) Expression of GFAP in astrocytes treated with high glucose after transfection with miR-125a-5p mimic. (D) Expression of MCP-1 in astrocytes treated with high glucose after transfection with miR-125a-5p mimic. \*\*, ##  $p < 0.01$ .

## Results

### MiR-125a-5p was reduced in diabetic mice

Type 2 diabetic mouse (db/db) was used as DPN model to evaluate the role of miR-125a-5p in peripheral neuropathy. The db/db mouse demonstrated higher blood glucose (Fig. 1A), higher body weight (Fig. 1B), lower mechanical allodynia (Fig. 1C) and thermal hyperalgesia (Fig. 1D) than db/m mouse, indicating that type 2 diabetic features of db/db mouse were accompanied by mechanical allodynia and thermal hyperalgesia. Moreover, astrocytic marker, GFAP, was increased in db/db mouse (Fig. 1E), suggesting the activation of astrocytes in the DPN model. The proinflammatory cytokine MCP-1 was also enhanced in db/db mice (Fig. 1F), suggesting inflammation activation in DPN model. MiR-125a-5p was reduced in spinal cord of db/db mice (Fig. 1G), indicating the potential regulatory role in DPN.

### MiR-125a-5p was decreased in high glucose-induced astrocytes

Primary astrocytes were prepared from cerebral cortexes of postnatal day 2 mice, and then treated with normal glucose or high glucose. High glucose treatment activated astrocytes by increasing GFAP (Fig. 2A). Moreover, MCP-1 was also increased in high glucose treated astrocytes (Fig. 2B). The reduction of miR-125a-5p in high glucose-induced astrocytes (Fig. 2C) might coincide with astrocytic activation involved in DPN.

### Forced miR-125a-5p repressed astrocytic activation post high glucose treatment

Astrocytes were transfected with miR-125a-5p mimic for two days and then treated with high glucose for 24 h before functional analysis. Compared with the NC mimic, higher miR-125a-5p expression was validated in astrocytes trans-

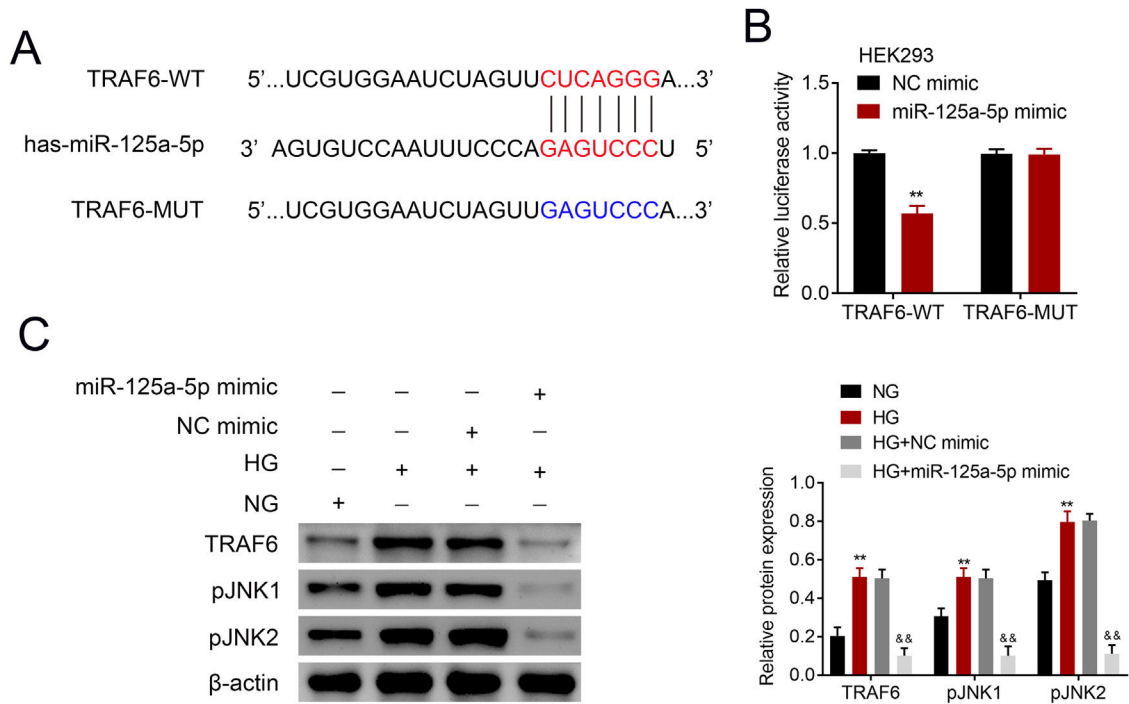


**Figure 4** MiR-125a-5p targeted TRAF6. (A) Potential binding site between miR-125a-5p and TRAF6. (B) Luciferase activity of TRAF6-WT and TRAF6-MUT affected by miR-125a-5p or NC mimic. (C) Expression of TRAF6, p-JNK1 and p-JNK2 in astrocytes post high glucose or normal glucose treatment, as well as expression of TRAF6, p-JNK1 and p-JNK2 in astrocytes treated with high glucose after transfection with miR-125a-5p mimic. \*\*, &&  $p < 0.01$ . TRAF6: tumor necrosis factor receptor associated factor 6; JNK: c-Jun N-terminal kinase.

ected with the mimic (Fig. 3A). Moreover, miR-125a-5p was also enhanced in astrocytes transfected with the mimic post high glucose treatment (Fig. 3B). Transfection with miR-125a-5p mimic reduced protein expression of GFAP (Fig. 3C) and MCP-1 (Fig. 3D) in high glucose-induced astrocytes, indicating that forced miR-125a-5p expression could repress astrocytic activation post high glucose treatment.

### MiR-125a-5p targeted TRAF6

The potential binding target of miR-125a-5p was predicted to be TRAF6 (Fig. 4A). To determine the targeting relationship between TRAF6 and miR-125a-5p, dual luciferase assay was performed. The results showed that forced miR-125a-5p expression reduced the luciferase activity of TRAF6-WT (Fig. 4B), while the luciferase activity of TRAF6-MUT whose binding site was mutated was not affected by miR-125a-5p mimic (Fig. 4B), demonstrating the binding ability between miR-125a-5p and 3'UTR of TRAF6. TRAF6 was up-regulated in high glucose-induced astrocytes (Fig. 4C), and high glucose could induce phosphorylation of JNKs with increased p-JNK1 and p-JNK2 in astrocytes (Fig. 4C). However, forced miR-125a-5p expression repressed the expression of TRAF6, p-JNK1 and p-JNK2 in astrocytes post high glucose treatment (Fig. 4C), suggesting that miR-125a-5p regulated astrocytic activation through TRAF6/JNK pathway.

### Forced miR-125a-5p repressed astrocytic activation in diabetic mice

The db/db mice were tail vein injected with miR-125a-5p mimic to determine effects of miR-125a-5p on DPN. Treatment of db/db mice with miR-125a-5p mimic demonstrated no significant change on blood glucose (Fig. 5A) and body weight (Fig. 5B) compared with NC mimic, indicating that the potential therapeutic effect miR-125a-5p on DPN was not dependent on reduction of hyperglycemia. However, the enhanced MWT (Fig. 5C) and TWL (Fig. 5D) in db/db mice after miR-125a-5p mimic treatment revealed that forced miR-125a-5p expression attenuated peripheral neuropathy in type 2 diabetic mice. MiR-125a-5p was enhanced in db/db mice post miR-125a-5p mimic treatment (Fig. 5E). Moreover, TRAF6, p-JNK1 and p-JNK2 were increased in db/db mice (Fig. 5F), while reduced in db/db mice post miR-125a-5p mimic treatment (Fig. 5F). Administration of miR-125a-5p mimic reduced the expression of MCP-1 (Fig. 5G) and GFAP (Fig. 5H) in db/db mice, revealing that forced miR-125a-5p expression might attenuate peripheral neuropathy through repression of astrocytic activation and inhibition of TRAF6/JNK pathway in diabetic mice.

### Discussion

Astrocytes are the most common type of glia in the central nervous system, and can be activated in chemotherapy-induced peripheral neuropathy rats.<sup>21</sup> Recently, astrocytic activation has been shown to be involved in mechanical

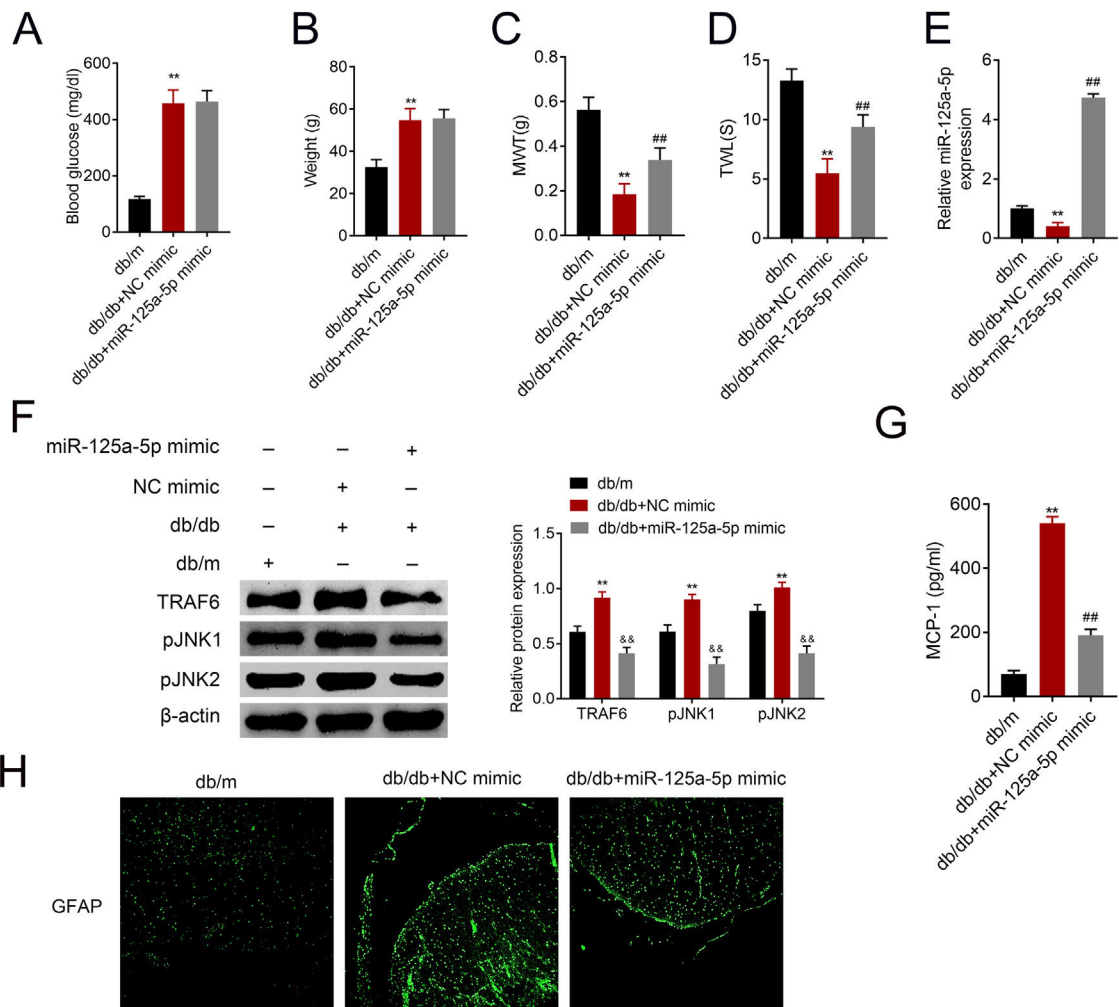


**Figure 5** Forced miR-125a-5p expression repressed astrocytic activation in diabetic mice. (A) Blood glucose in db/m, db/db and db/db mice injected with miR-125a-5p mimic. (B) Body weight of db/m, db/db and db/db mice injected with miR-125a-5p mimic. (C) Mechanical allodynia of db/m, db/db and db/db mice injected with miR-125a-5p mimic detected by MWT. (D) Thermal hyperalgesia of db/m, db/db and db/db mice injected with miR-125a-5p mimic detected by TWL. (E) Expression of miR-125a-5p in spinal cord of db/m, db/db and db/db mice injected with miR-125a-5p mimic detected by qRT-PCR. (F) Expression of TRAF6, p-JNK1 and p-JNK2 in db/m, db/db and db/db mice injected with miR-125a-5p mimic. (G) MCP-1 in db/m, db/db and db/db mice injected with miR-125a-5p mimic detected by ELISA. (H) Immunofluorescence of GFAP in spinal cord of db/m, db/db and db/db mice injected with miR-125a-5p mimic. \*\*, ##  $p < 0.01$ .

allodynia threshold of type 2 diabetic mice.<sup>22</sup> Considering that miR-125a-5p, found in astrocyte derived extracellular vesicles, can regulate neurotrophic pathway and thus participate in the pathogenesis of neurodegenerative disorders,<sup>23</sup> the role of miR-125a-5p in DPN in type 2 diabetic mice was evaluated in this study.

The db/db mouse, with a null mutation on leptin receptor, exhibits type 2 diabetic phenotypes, including hyperglycemia and hyperlipidemia, and imitates the chronic pain state in human.<sup>24</sup> Therefore, db/db mouse is widely used as DPN model.<sup>24</sup> Results in the present study showed that db/db mouse demonstrated higher blood glucose and body weight. Moreover, since DPN was manifested as allodynia threshold and hyperalgesia,<sup>25</sup> the sensitivities of db/db mice to normally painful stimuli were validated as lower mechanical allodynia threshold and thermal hyperalgesia. These findings revealed that db/db mouse demonstrated

hyperglycemia feature that coincided with mechanical allodynia threshold and thermal hyperalgesia. In addition, the astrocytic activation marker GFAP was also increased in db/db mice. MCP-1, secreted by activated astrocyte, could increase pain sensitivity and enhance the persistent pain states.<sup>26</sup> Our result also demonstrated higher MCP-1 expression in db/db mouse compared with db/m mouse.

A previous study has shown that miR-125a-5p was not co-labeled with GFAP in ventral horn of experimental autoimmune encephalomyelitis mice.<sup>12</sup> However, reduction of miR-125a-5p was found in spinal cord of db/db mice and high glucose-induced astrocytes. High glucose was reported to increase GFAP level in retinal astrocytes<sup>27</sup> or MCP-1 in microglia,<sup>28</sup> thereby regulating DPN or diabetic encephalopathy. Here, our results showed that high glucose induced astrocytic activation and increased GFAP and MCP-1. Further functional assays indicated that forced

miR-125a-5p expression decreased GFAP and MCP-1 expression to suppress astrocytic activation, suggesting the potential role in DPN. Astrocytic activation has been shown to promote mechanical allodynia threshold in type 2 diabetic mice,<sup>22</sup> and increase in thermal hyperalgesia and mechanical allodynia threshold could attenuate DPN in rats.<sup>29</sup> Our results showed that tail vein injection of miR-125a-5p mimic into db/db mice increased thermal hyperalgesia and mechanical allodynia threshold, and decreased GFAP and MCP-1, thereby suppressing astrocytic activation and attenuating of DPN in mice.

TRAF6, regulated by cytokine and toll-like receptors, can mediate NF- $\kappa$ B pathway to participate in progression of inflammation-related diseases, including diabetes mellitus.<sup>16</sup> High glucose can induce TRAF6 through activation of JNK pathway.<sup>16</sup> Moreover, up-regulation of TRAF6 in astrocytes maintains neuropathic pain by activation of JNK/MCP-1 pathway.<sup>30</sup> Therefore, down-regulation of TRAF6 by miR-146a has been shown to reduce peripheral neuropathy in db/db mice.<sup>7</sup> Data from this study revealed that forced miR-125a-5p in astrocytes decreased TRAF6, p-JNK1 and p-JNK2 to suppress astrocytic activation. In addition, administration of miR-125a-5p mimic also decreased TRAF6, p-JNK1 and p-JNK2 to attenuate DPN in db/db mice. However, since TRAF6 is also involved in miR-146a-mediated inflammation in type 2 diabetic rats,<sup>6</sup> whether TRAF6/NF- $\kappa$ B is involved in miR-125a-5p-mediated DPN needs to be further investigated. Moreover, the lack of blinding was considered as the limitation of this study.

In conclusion, our results demonstrated that elevation of miR-125a-5p in db/db mice suppressed astrocytic activation, and improved sensitivity to normally painful stimuli, thereby providing a permissive restorative to ameliorate DPN.

## Availability of data and materials

All data generated or analyzed during this study are included in this published article.

## Ethics approval

Ethical approval was obtained from the Ethics Committee of People's Hospital of Xinjiang Uygur Autonomous Region

## Funding

This research did not receive any specific grant from funding agencies in the public, commercial, or not-for-profit sectors.

## Authors' contributions

Aziguli Kasimu and Xierenguli Apizi designed the study, supervised the data collection, Dilibaier Talifujiang analyzed the data, interpreted the data, Xin Ma, Liping Fang and Xiangling Zhou prepare the manuscript for publication and reviewed the draft of the manuscript. All authors have read and approved the manuscript.

## Conflict of interest

The authors state that there are no conflicts of interest to disclose.

## References

- Davies M, Brophy S, Williams R, Taylor A. The prevalence, severity, and impact of painful diabetic peripheral neuropathy in type 2 diabetes. *Diabetes Care*. 2006;29:1518–22, <http://dx.doi.org/10.2337/dc05-2228>.
- Singh R, Kishore L, Kaur N. Diabetic peripheral neuropathy: current perspective and future directions. *Pharmacol Res*. 2014;80:21–35, <http://dx.doi.org/10.1016/j.phrs.2013.12.005>.
- Vanotti A, Osio M, Mailland E, Nascimbene C, Capiluppi E, Mariani C. Overview on pathophysiology and newer approaches to treatment of peripheral neuropathies. *CNS Drugs*. 2007;21 Suppl. 1:3–12, <http://dx.doi.org/10.2165/00023210-200721001-00002>, discussion 45–6.
- Liang JXY, Liu L, Qiao L, Peng P, Zhou J. Combined measurement of miRNA-183, HE4, and CA-125 increases diagnostic efficiency for ovarian cancer. *Eur J Gynaecol Oncol*. 2020;41:30–5, <http://dx.doi.org/10.31083/j.ejgo.2020.01.4788>.
- Xourgia E, Papazafropoulou A, Melidonis A. Circulating microRNAs as biomarkers for diabetic neuropathy: a novel approach. *World J Exp Med*. 2018;8:18–23, <http://dx.doi.org/10.5493/wjem.v8.i3.18>.
- Feng Y, Chen L, Luo Q, Wu M, Chen Y, Shi X. Involvement of microRNA-146a in diabetic peripheral neuropathy through the regulation of inflammation. *Drug Des Dev Ther*. 2018;12:171–7, <http://dx.doi.org/10.2147/DDDT.S157109>.
- Liu XS, Fan B, Szalad A, Jia L, Wang L, Wang X, et al. MicroRNA-146a mimics reduce the peripheral neuropathy in type 2 diabetic mice. *Diabetes*. 2017;66:3111–21, <http://dx.doi.org/10.2337/db16-1182>.
- Zhang Y, Song C, Liu J, Bi Y, Li H. Inhibition of miR-25 aggravates diabetic peripheral neuropathy. *Neuroreport*. 2018;29:945–53, <http://dx.doi.org/10.1097/WNR.0000000000001058>.
- Xu X, Tao Y, Niu Y, Wang Z, Zhang C, Yu Y, et al. miR-125a-5p inhibits tumorigenesis in hepatocellular carcinoma. *Aging*. 2019;11:7639–62, <http://dx.doi.org/10.18632/aging.102276>.
- Tong Z, Liu N, Lin L, Guo X, Yang D, Zhang Q. miR-125a-5p inhibits cell proliferation and induces apoptosis in colon cancer via targeting BCL2, BCL2L1 and MCL1. *Biomed Pharmacother*. 2015;75:129–36, <http://dx.doi.org/10.1016/j.biopha.2015.07.036>.
- Cao Q, Wang N, Ren L, Tian J, Yang S, Cheng H. miR-125a-5p post-transcriptionally suppresses GALNT7 to inhibit proliferation and invasion in cervical cancer cells via the EGFR/PI3K/AKT pathway. *Cancer Cell Int*. 2020;20:117, <http://dx.doi.org/10.1186/s12935-020-01209-8>.
- Long HC, Wu R, Liu CF, Xiong FL, Xu Z, He D, et al. MiR-125a-5p regulates vitamin D receptor expression in a mouse model of experimental autoimmune encephalomyelitis. *Neurosci Bull*. 2020;36:110–20, <http://dx.doi.org/10.1007/s12264-019-00418-0>.
- Xu L, Li Y, Yin L, Qi Y, Sun H, Sun P, et al. miR-125a-5p ameliorates hepatic glycolipid metabolism disorder in type 2 diabetes mellitus through targeting of STAT3. *Theranostics*. 2018;8:5593–609, <http://dx.doi.org/10.7150/thno.27425>.
- Wu H, Arron JR. TRAF6, a molecular bridge spanning adaptive immunity, innate immunity and osteoimmunology. *BioEssays*. 2003;25:1096–105, <http://dx.doi.org/10.1002/bies.10352>.

15. Zeng C, Zhou Z, Han Y, Wen Z, Guo C, Huang S, et al. Interactions of TRAF6 and NLRX1 gene polymorphisms with environmental factors on the susceptibility of type 2 diabetes mellitus vascular complications in a southern Han Chinese population. *J Diabetes Complic.* 2017;31:1652–7, <http://dx.doi.org/10.1016/j.jdiacomp.2017.08.013>.
16. Liu R, Shen H, Wang T, Ma J, Yuan M, Huang J, et al. TRAF6 mediates high glucose-induced endothelial dysfunction. *Exp Cell Res.* 2018;370:490–7, <http://dx.doi.org/10.1016/j.yexcr.2018.07.014>.
17. Wang L, Chopp M, Szalad A, Zhang Y, Wang X, Zhang RL, et al. The role of miR-146a in dorsal root ganglia neurons of experimental diabetic peripheral neuropathy. *Neuroscience.* 2014;259:155–63, <http://dx.doi.org/10.1016/j.neuroscience.2013.11.057>.
18. Wang L, Chopp M, Lu X, Szalad A, Jia L, Liu XS, et al. miR-146a mediates thymosin  $\beta$ 4 induced neurovascular remodeling of diabetic peripheral neuropathy in type-II diabetic mice. *Brain Res.* 2019;1707:198–207, <http://dx.doi.org/10.1016/j.brainres.2018.11.039>.
19. Wang W, Guo Z-H. Downregulation of lncRNA NEAT1 ameliorates LPS-induced inflammatory responses by promoting macrophage M2 polarization via miR-125a-5p/TRAF6/TAK1 axis. *Inflammation.* 2020.
20. Rasheed Z, Rasheed N, Abdulmonem ALW, Khan MI. MicroRNA-125b-5p regulates IL-1 $\beta$  induced inflammatory genes via targeting TRAF6-mediated MAPKs and NF- $\kappa$ B signaling in human osteoarthritic chondrocytes. *Sci Rep.* 2019;9:1–13.
21. Robinson CR, Zhang H, Dougherty PM. Astrocytes, but not microglia, are activated in oxaliplatin and bortezomib-induced peripheral neuropathy in the rat. *Neuroscience.* 2014;274:308–17, <http://dx.doi.org/10.1016/j.neuroscience.2014.05.051>.
22. Liao YH, Zhang GH, Jia D, Wang P, Qian NS, He F, et al. Spinal astrocytic activation contributes to mechanical allodynia in a mouse model of type 2 diabetes. *Brain Res.* 2011;1368:324–35, <http://dx.doi.org/10.1016/j.brainres.2010.10.044>.
23. Chaudhuri AD, Dastgheyb RM, Yoo SW, Trout A, Talbot CC Jr, Hao H, et al. TNF $\alpha$  and IL-1 $\beta$  modify the miRNA cargo of astrocyte shed extracellular vesicles to regulate neurotrophic signaling in neurons. *Cell Death Dis.* 2018;9:363, <http://dx.doi.org/10.1038/s41419-018-0369-4>.
24. Cheng HT, Dauch JR, Oh SS, Hayes JM, Hong Y, Feldman EL. p38 mediates mechanical allodynia in a mouse model of type 2 diabetes. *Mol Pain.* 2010;6:28, <http://dx.doi.org/10.1186/1744-8069-6-28>.
25. Barrett AM, Lucero MA, Le T, Robinson RL, Dworkin RH, Chappell AS. Epidemiology, public health burden, and treatment of diabetic peripheral neuropathic pain: a review. *Pain Med.* 2007;8 Suppl. 2:S50–62, <http://dx.doi.org/10.1111/j.1526-4637.2006.00179.x>.
26. Gao Y-J, Ji R-R. Targeting astrocyte signaling for chronic pain. *Neurotherapeutics.* 2010;7:482–93, <http://dx.doi.org/10.1016/j.nurt.2010.05.016>.
27. Shin ES, Huang Q, Gurel Z, Sorenson CM, Sheibani N. High glucose alters retinal astrocytes phenotype through increased production of inflammatory cytokines and oxidative stress. *PLOS ONE.* 2014;9, <http://dx.doi.org/10.1371/journal.pone.0103148>, e103148-e.
28. Quan Y, Jiang C-t, Xue B, Zhu S-g, Wang X. High glucose stimulates TNF $\alpha$  and MCP-1 expression in rat microglia via ROS and NF- $\kappa$ B pathways. *Acta Pharmacol Sin.* 2011;32:188–93, <http://dx.doi.org/10.1038/aps.2010.174>.
29. Chen YW, Hsieh PL, Chen YC, Hung CH, Cheng JT. Physical exercise induces excess hsp72 expression and delays the development of hyperalgesia and allodynia in painful diabetic neuropathy rats. *Anesth Analg.* 2013;116:482–90, <http://dx.doi.org/10.1213/ANE.0b013e318274e4a0>.
30. Lu Y, Jiang B-C, Cao D-L, Zhang Z-J, Zhang X, Ji R-R, et al. TRAF6 upregulation in spinal astrocytes maintains neuropathic pain by integrating TNF- $\alpha$  and IL-1 $\beta$  signaling. *Pain.* 2014;155:2618–29, <http://dx.doi.org/10.1016/j.pain.2014.09.027>.